Natural Hazards (2024) 120:11987–12010
https://doi.org/10.1007/s11069-024-06670-6

ORIGINAL PAPER

Development of risk maps for flood, landslide, and soil erosion using machine learning model

Narges Javidan[1] · Ataollah Kavian[1] · Christian Conoscenti[2] · Zeinab Jafarian[3] · Mahin Kalehhouei[4] · Raana Javidan[5,6]

Received: 1 January 2024 / Accepted: 6 May 2024 / Published online: 9 June 2024

Abstract
Natural hazards, such as flood, landslide, and erosion, are the reality of human life. spatial prediction of these hazards and their effectiveness factors are extremely important. The main goal of this study was to prepare multi-hazard probability mapping (flood, landslide, and gully erosion) of the Gorganrood Watershed. In addition, different machine learning models such as Random Forest (RF), Support Vector Machine (SVM), Boosted Regression Tree (BRT), and Multivariate Adaptive Regression Spilines (MARS) were applied. First, a flood, landslide, and gully erosion inventory map was produced using GPS in the field surveys and Google Earth. Factors affecting the hazards were identified, and GIS maps were prepared. The MARS model (AUC = 99.1%) provided the highest predictive performance for flood, landslide, and gully erosion hazards. However, for flood and landslide, the RF model exposed excellent and good performance, respectively. According to the variable importance analysis, drainage density (89.4%), digital elevation model (30.5%), and rainfall (41.7%) were consistently highly ranked variables for flood, landslide, and gully erosion, respectively. Multi-hazard maps can be a valuable tool for the conservation of natural resources and the environment, as well as for sustainable land use planning in multi-hazard-prone areas.

Keywords Machine learning models · Multi-hazard probability mapping · Natural hazards · Receiver operating characteristic · Spatial prediction

1 Introduction

A natural hazard is a kind of unexpected shock that causes social and economic damage to the environment and human life (Gill and Malamud 2014; Karaman 2015; Kourtit et al. 2023). In recent years, the impact of natural disasters has increased. Man-made human activities are also one of the main factors that may affect degradation processes (Kavian et al. 2017; Ge et al. 2021). In order to mitigate the threat of natural hazards and improve risk management, a UN flowchart has strongly highlighted the identification of multi-hazard zones (Pourghasemi et al. 2019; Widantara and Mutaqin 2024). Many parts of Iran are susceptible to a variety of devastating disasters. Numerous

Extended author information available on the last page of the article

hazards such as flood, landslide, and erosion have seriously affected Northern Iran in multiple ways (Kornejady et al. 2017; Islam et al. 2021). These basic problems are known as natural hazards because they jeopardize nature and human life (Soulard et al. 2016; Al Mamun et al. 2023). The average annual economic loss due to flood and landslide is approximately $1.705.000 (Norouzi and Taslimi 2012). Acceleration of flooding caused by irresponsible human activities (Moghaddam et al. 2019; Nyantakyi-Frimpong et al. 2023). Most areas in northern Iran are also affected by gully erosion and landslide (WRCG 2013). The Gorganrood watershed in Golestan province was chosen as the study area due to its history of disasters such as flood, landslide, and erosion (Kavian et al. 2023). The region has experienced significant damage and loss of life due to natural hazards, including a devastating flood in August 2019, which resulted in numerous casualties and extensive financial damage. The prevalence of land use practices contribute to flood production capacity and erosion, coupled with the presence of steep lands prone to landslides, makes the Gorganrood watershed a critical area for hazard mapping and risk assessment studies. By focusing on this region, researchers aim to better understand and mitigate the impacts of these hazards, contributing to disaster preparedness and prevention efforts in Golestan province and beyond. However, flooding, landslides, and erosion are complex events that occur topographically in different places (Shi et al. 2023). In addition, natural events have different effects on different elements of hazardous processes; therefore, it is possible to map the distributions of their occurrence in a single map. The fundamental requirement for a Multi-Hazard-Map (MHM) as a proper tool in a situation where a region is exposed to more than one event (Sheikh et al. 2019) which can be very useful and valuable for the decision makers, local administrators and hazard managers (Pourghasemi et al. 2019; Sari 2023). In addition, identifying priority zones in the form of MHM is crucial for prognosticating potential impacts (UNEP 1992).

Many previous studies have used machine learning (MLe) algorithm as a single susceptibility phenomenon map to determine floods (Khosravi et al. 2016; Brito et al. 2018; Arabameri et al. 2019; Moghaddam et al. 2019; Costache et al. 2020, 2024; El-Magd and Ahmed; 2022; Hai et al. 2023), gully erosion (Conforti et al. 2011; Conoscenti et al. 2013, 2014; Gayen et al. 2020; Wang et al. 2022; Raji et al. 2023; Li et al. 2024) and landslides areas (Marjanović et al. 2011; Micheletti et al. 2014; Chen et al. 2017; Sameen et al. 2020; Alqadhi et al. 2022; Ganesh et al. 2023; Nanda et al. 2024). The spatial anticipation of an occurrence is known as susceptibility, which is defined as the link between the impressive environmental parameters and the event samples (sheikh et al. 2019). However, several hazards can occur simultaneously in one area. Multi-hazard potentiality map (MHPM) illustrates susceptibility and potentiality information of a region, on a single united map (Pourghasemi et al. 2019). The study of MHM as an integrated approach was recently enhanced (Komac 2006; El Morjani 2007; Karaman 2015; Bathrellos et al. 2017; Pourghasemi et al. 2018, 2019; Aksha et al. 2020).

Random Forest (RF), Support Vector Machine (SVM), Boosted Regression Tree (BRT), and Multivariate Adaptive Regression Splines (MARS) are the most popular types of machine learning that can forecast flood, landslide, and gully erosion in the areas at risk (Hong et al. 2015; Bui et al. 2016b; Youssef et al. 2016; Zhao et al. 2018; Kalantar et al. 2018; Avand et al. 2019; Javidan et al. 2020). Random Forest model is an ensemble learning method that operates by constructing multiple decision trees

during training and outputs the mode of the classes or mean prediction of the individual trees. It is known for its high accuracy, robustness to overfitting, and capability to handle large datasets with high dimensionality (Gayen et al. 2020). SVM is a supervised learning algorithm used for classification and regression tasks. It works by finding the hyperplane that best separates the classes in the feature space. SVM is effective for high-dimensional data and in cases where the data is not linearly separable (Marjanović et al. 2011). Boosted Regression Tree is a machine learning technique that combines the power of regression trees with boosting, a method of building models sequentially to reduce prediction errors. It is known for its ability to handle complex interactions in the data and provide high predictive accuracy (Youssef et al. 2016). MARS is a non-parametric regression technique that models the relationship between predictors and the target variable as a series of piecewise linear segments (Conoscenti et al. 2013, 2014). It is suitable for capturing nonlinear relationships in the data and can handle interactions between variables effectively.

on the other handnot yet specified which of these accurate models is the best for developing an MHM. It is undeniable that it is possible to predict which areas are at risk, such as flooding, landslides or gully erosion.

To address this considerable study gap, RF, SVM, BRT, and MARS methods were used as benchmarks to determine which of these accurate models is the best to develop an MHM. This study goes beyond traditional hazard assessment methods by employing a range of machine learning models. The thorough comparison of these models and the identification of the most effective one for predicting multi-hazard probabilities demonstrate the innovative application of advanced techniques in hazard mapping. By integrating the modeling of multiple hazards into a single framework, our study offers a more holistic understanding of the combined risks faced by the region, which can be crucial for effective disaster risk management and land use planning. By emphasizing the practical implications of multi-hazard mapping for natural resource conservation, environmental protection, and sustainable land use planning, this study offers valuable insights for decision-makers and stakeholders involved in mitigating risks associated with multiple hazards in the Gorganrood Watershed. The potential for using multi-hazard maps as a tool for enhancing resilience and preparedness in hazard-prone areas further underscores the innovative and impactful nature of this research. It is undisputed which zones are prone to multi-natural disasters such as flood (F), landslide (L), or gully erosion (Ge) (FLGe). Thus, the current research paper was conducted in the Gorganrood watershed, which is highly predisposed to three natural phenomena such as FLGe with these targets: (1) Compare the accuracy of different machine learning methods (Random Forest, Support Vector Machine, Boosted Regression Tree, and Multivariate Adaptive Regression Splines) in creating sensitivity maps for each hazard (flood, landslide, gully erosion), (2) Developing a MHPM based on the output maps from the best hazard predictor model, (3) Identifying zones prone to multiple hazards using the best-performing method. These objectives aim to address the complex mechanisms and various factors influencing the occurrence of flood, landslide, and gully erosion. By pinpointing high-risk areas, this research can assist land managers and planners in implementing effective land management and development strategies.

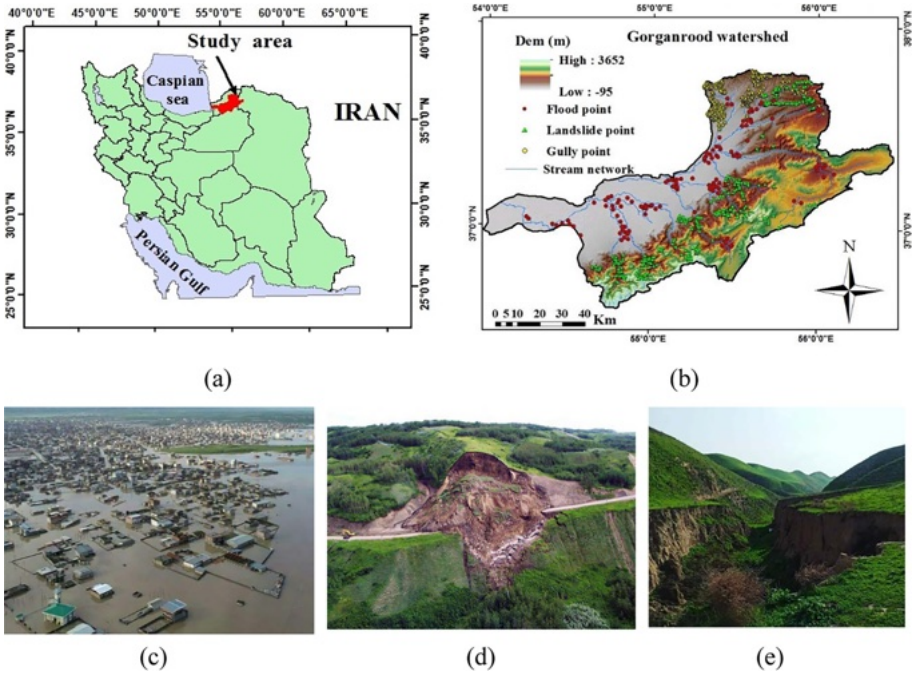

Fig. 1 Location of the study area in the province of Golestam and Iran (**a**), sampling points and elevation (**b**), View of flood (**c**), landslide (**d**) and gully erosion (**e**) in Golestan Province

2 Material and methods

2.1 Study area

The Gorganrood watershed is located in the northeastern part of Iran between latitudes of 36° 35′ and 38° 15′ N and longitudes of 45° 10′ and 56° 26′ E. The study area occupies nearly 10.197 km^2 (Fig. 1) and is elevated from 95 to 3.652 m a.s.l. The southern part of the region has a mountainous morphology with steep slopes (up to 69°), whereas the northern part has deserts and flat areas. The central areas are climatologically categorized as mainly the Mediterranean (Sheikh et al. 2019). The annual mean precipitation is approximately 454 mm per year, with average temperatures of approximately 11–18.5 °C in winter and summer, respectively (Conrwmgp 2009). The main land cover category in this region is agricultural land with an area of approximately 4390 km^2. Some hazard-prone lithological formations include the Dalichay, Durod, Shemshak, Mobarak, and Alluvial terraces. Approximately 59% of this area is covered by Quaternary sediment. In recent years, this region has experienced multiple natural phenomena such as flood, landslide, and erosion due to blind development, deforestation, climate conditions, and diverse geology. Therefore, this area was chosen as a case study for multi-hazard potentiality evaluation (MHPE) (Fig. 1).

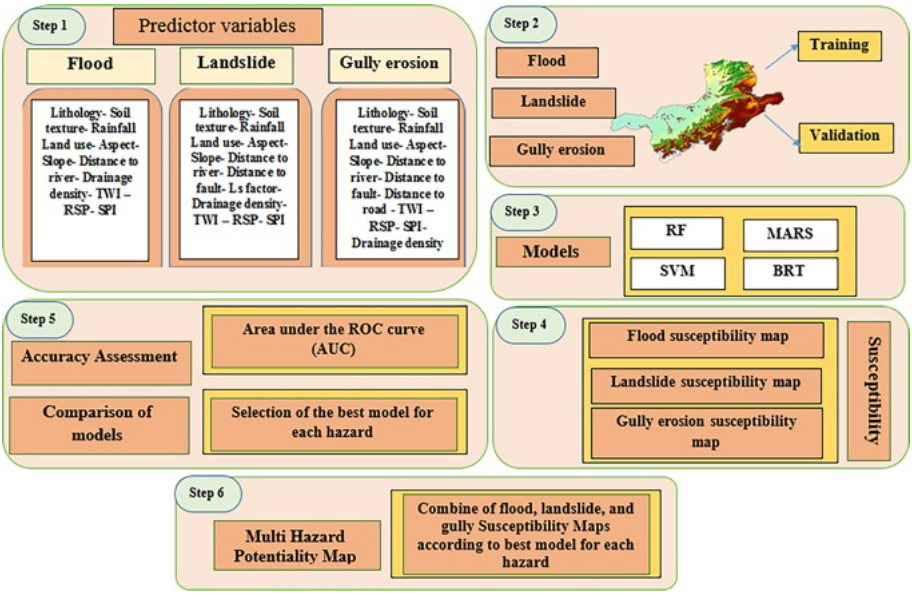

Fig. 2 Methodological flowchart for the study of Multi-Hazard

2.2 2–2 Methodology

Figure 2 presents a flowchart of the different stages of multiple hazard mapping, modeling, and preparation of FLGe susceptibility mapping using data mining techniques and statistical models. Due to the critical nature of the natural hazards of the Gorganrood watershed, most parts of this area were visited in the field and eventually selected as a search area.

2.2.1 Preparing predictor variable base maps

Several geological maps at scale 1:100,000 were used to identify the geological features of the study area and develop a lithological map. The Golestan Watershed Management Department developed land use map of the study area using Landsat satellite imagery. The ETM $^{+}$ 2008 images from the GLOVIS[1] site were used in the analysis of satellite images. The map has been modified as a result of field studies and adaptation to the land-use reality in the region, Google Earth images and satellite images. A digital elevation model of the study area was prepared from the Department of Natural Resources and Watershed Management of Golestan Province and obtained by using topographic maps at a scale of 1:25,000 with a spatial resolution of 30×30 m.

Factors affecting hazard susceptibility in the study area were prepared using ArcGIS10.5 and SAGA software and turned into raster layers with a spatial resolution of 30×30 m. Commonly used predictors for the three hazards of FLGe include digital elevation model (m), slope direction, slope percentage, slope longitudinal curvature (SLC), transverse slope curvature (TSC), land use, soil texture, slope length factor, topographic

[1] The USGS Global Visualization Viewer.

wetness index (TWI), distance from stream network (m), drainage density, annual rainfall (mm), stream power index (SPI) relative slope position (RSP), Melton roughness coefficient, lithological formations, distance from road (m), and distance from the fault (m) (Fig. 3). The last two factors were not used for the flood. After preparing the layers, SPSS software was used to analyze the alignment data. Alignment can be properly judged by controlling the tolerance thresholds and variance inflation factor (VIF) (Greene 2000).

In addition, VIF is the reverse tolerance threshold (Daoud 2017). A disposal sensitivity analysis and a JackKnife test of the maximum entropy model were used to determine the impact of environmental variables on the occurrence of each hazard. After preparing the information layers, the factors affecting each risk were classified using the natural breaking method, and the percentage of FLGe risks in each categorywas determined. The hazard frequency in each categorization was then obtained using the overlap of the hazard distribution map with each factorial layer. The correct weight for each category is computed using this method.

2.2.2 Preparation of a FLGe risk distribution map in the case study

Preparing a distribution map of point of occurrence is a key step in the preparation of a sensitivity map (Conoscenti et al. 2014; Gnyawali et al. 2023). FLGe hazards have been studied in field studies and surveys and their geographical location has been recorded using a GPS[2] global positioning device. Geological formations, road construction, land-use change, and inadequate slope conversion and tillage have been the major causes of these hazards in the study area. The locations of 283. 351 landslide, and 127 flood points were recorded, and a distribution map of the locations of these hazards was prepared in ArcGIS10.5 software. A random partition algorithm was used to segregate training points from validation points (Rahmati et al. 2016). Finally, 70% of participants were selected as a training group and the remaining 30% as the validation group.

2.2.3 Multi-hazards modeling using data mining models

Various machine learning models, including Random Forest (RF), Support Vector Machine (SVM), Boosted Regression Tree (BRT), and Multivariate Adaptive Regression Splines (MARS), were also implemented to establish the spatial relationship between these hazards and the geo-environmental factors (GEFs) and any hazard susceptibility mapping separately. Finally, to determine the best multi-hazard map, the evaluation of multi-hazard mapping with different combinations of multi-hazard maps was done.

2.2.4 Susceptibility map

Preparation of a distribution map of occurrence points is a key step in preparing a sensitivity map (Conoscenti et al. 2014). Depending on the purpose and accessibility of the data, the natural hazard distribution map includes two categories: local scale and national scale, which were prepared by various techniques such as aerial photo interpretation, geomorphological studies, satellite imagery, past events, and field surveys (Guzzetti et al. 2000). A susceptibility map of each hazard in the GIS was prepared for this purpose.

[2] Global Positioning System.

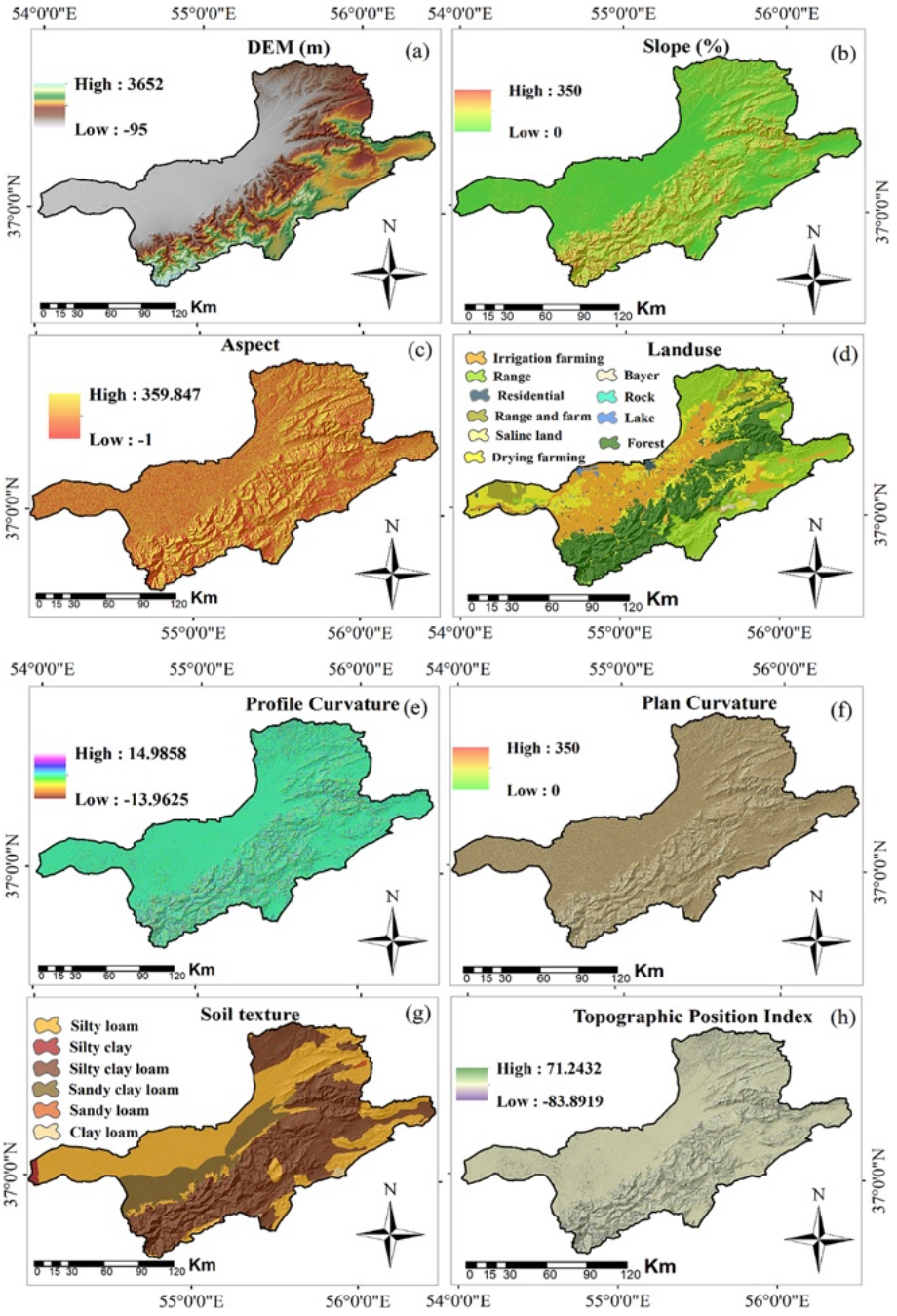

Fig. 3 Maps displaying the FLGe conditioning factors: **a** DEM (m), **b** Slope percent **c** Slope aspect, **d** Land use, **e** Profile curvature (g), **f** Plan curvature, **g** Soil texture, **h** Topographic Position Index (TPI) **i** Topographic Wetness Index (TWI), **j** Distance to streams (m), **k** Drainage density (km/km^2), **l** Annual mean rainfall (mm), **m** Stream Power Index, **n** Relative Slope Position, **o** Terrain Ruggedness Index, **p** Lithology**,** **q** LS factor**,** **r** Distance to road (m), **s** Distance to faults (m)

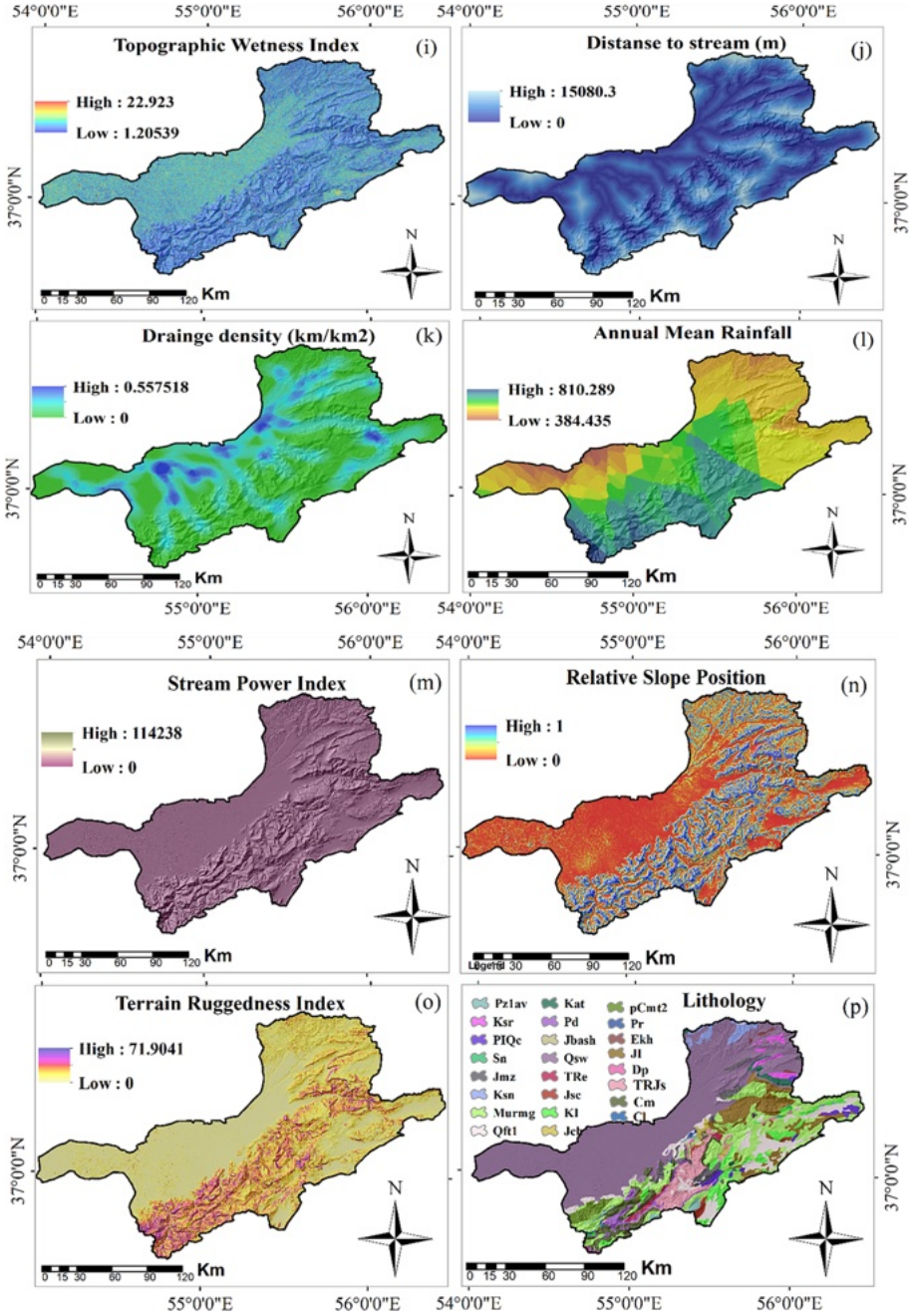

Fig. 3 (continued)

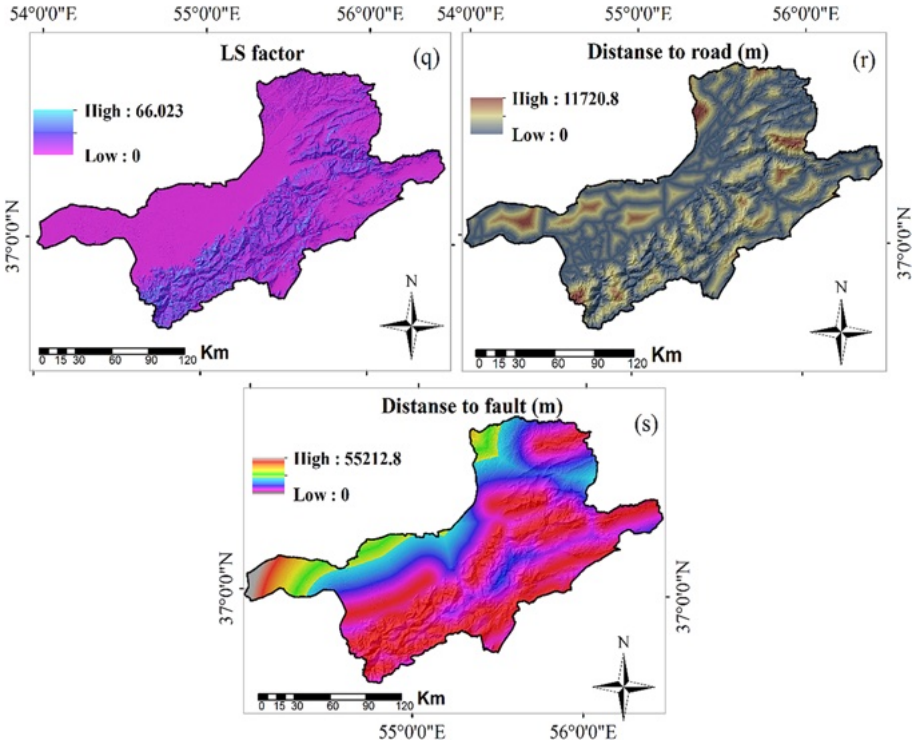

Fig. 3 (continued)

2.2.5 Evaluation of multi-hazard model predictive performance

At this stage, FLGe hazards were modeled based on the occurrence of validation group hazards (30% of past events) using the receiver operating characteristic curve (ROC) method for all the models used. The area under this curve (AUC) is used as a quantitative measure for validation (FelicÍsimo et al. 2013). The accuracy of the model will be acceptable if the area under the curve is greater than 70% (Yesilnacar 2005). For qualitative and quantitative correlations below the curve and estimation estimates were used, divide 0.9–1 excellent, 0.8–0.9 very good, 0.7–0.8 good, 0.6–0.7 moderate and 0.6–0.5 poor (Yesilnacar and Topal 2005; Devkota 2013). At this stage, we compared the performance of all the models used (RF, SVM, BRT, and MARS) to determine the favorable areas for these hazards. The ROC curve axes were obtained based on the criteria of sensitivity and detection. Finally, we identify the most appropriate and superior model (in terms of precision, time, and data needed for simulation).

2.2.6 Multi hazard potentiality map

The best hazard map model was selected after determining the efficiency and accuracy of each hazard map using different models. This method determines which model is most suitable for preparing a flood risk map or any other individual risk. Subsequently, the superior

methods of each hazard were combined. A multi-hazard susceptibility map was obtained using ArcGIS tool by integrating the susceptibility map related to FLGe hazards by combining different methods. The final map was classified for each model for each hazard using the natural breaking method. By combining these three maps and executing a combined command, these three maps became multiple hazard maps with eight classes. This multi-hazard map includes a map resulting from a combination of superior and selected models of each hazard, as well as a combination of other methods used to prepare a single hazard map.

3 Results

According to Table 1, Terrain Ruggedness Index (TRI) for FLGe with VIF > 5 and tolerance < 0.1 was eliminated. Therefore, other factors will be used for future analyses, and the results show no multi-collinearity among the remaining independent variables in the present study. Figures 4, 5, and 6 show the FLGe susceptibility maps produced using the RF, SVM, BRT, and MARS models in four categories: low (L), moderate (M), high (H), and very high (VH) based on the output susceptibility maps using the most authentic natural break classifying method. The RF model revealed that sloping and highland areas have high and low occurrence potentials for landslide and gully erosion, respectively, and alluvial and flat central parts adjacent to surface currents have a moderate to high potential for flood risk. The SVM model shows that alluvial and flat central areas are prone to floods and erosion, respectively, and sloping and highland areas are also prone to landslide. On the basis of the BRT model, sloping, high, and away from surface currents have low and moderate susceptibility to floods and gully erosion and high susceptibility to landslide. Central flat sections adjacent to surface currents and susceptible soils have a high potential for flooding and gully erosion. In addition, there is a high probability of landslide in a large area of the region (43%). Finally, the MARS model shows that the steep parts of the study area are more prone to landslide.

Figure 7 shows the relative distribution of the mean classes of FLGe susceptibility maps for the four models: RF, SVM, BRT, and MARS. On the basis of these results for flood susceptibility classes, most classes of models FR, MARS, and BRT are in the low range, and SVM models are in the moderate range. According to landslide susceptibility classes, most classes of FR, SVM, and MARS models are in the low range, whereas the BRT model is in the high range. The gully erosion susceptibility classes showed that most of the models FR, BRT, SVM, and MARS are in the low range. Table 2 shows the statistical characteristics of the probabilistic prediction of the three hazards obtained from RF, SVM, BRT, and MARS models.

The validation of multi-hazard area forecast maps is illustrated in Fig. 8 and Table 3. On the basis of these results, the MARS model had the highest accuracy for flooding (AUC = 99.1), landslide (AUC = 87.4), and gully erosion risk (AUC = 98.5). The RF model for floods (AUC = 97.2) and landslide (AUC = 82.9) had the most accuracy.

Comparing different methods and determining the best method for each risk and combining different and superior methods for preparing multi-hazard sensitivity maps showed that the MARS model is the best model for mapping any hazard (Figs. 9 and 10). Accordingly, the maximum and minimum areas are related to no hazard (46.43%) and three combined hazards FLGe (0.55%), respectively. Table 4 shows the results of validation of the MARS model for FLGe hazard based on the kappa coefficient and statistical characteristics

Table 1 The results of multi-collinearity test

Predictors of floods	Collinearity statistics		Predictors of landslide	Collinearity statistics		Predictors of gully erosion	Collinearity statistics	
	Tolerance	VIF		Tolerance	VIF		Tolerance	VIF
Drainage density	0.386	2.589	Plan curvature	0.729	1.372	Plan curvature	0.639	1.564
Relative slope position	0.694	1.442	Annual mean rainfall	0.610	1.641	Annual mean rainfall	0.580	1.723
Slope	0.210	4.752	Drainage density	0.334	2.997	Drainage density	0.385	2.598
Soil	0.788	1.269	Relative slope position	0.328	1.592	Relative slope position	0.616	1.624
Stream power index	0.734	1.362	Slope percent	0.394	2.538	Slope percent	0.358	2.793
Topographic wetness index	0.656	1.525	Soil texture	0.880	1.136	Soil texture	0.772	1.296
Elevation	0.454	2.205	Stream power index	0.241	4.156	Stream power index	0.400	2.500
Distance to stream	0.428	2.335	Elevation	0.451	2.215	Topographic Wetness Index	0.557	1.796
Land use	0.902	1.109	Distance to fault	0.804	1.244	Aspect	0.943	1.060
lithology	0.687	1.455	Distance to stream	0.311	3.217	Elevation	0.427	2.342
Plan curvature	0.634	1.576	Land use	0.857	1.167	Distance to road	0.733	1.364
Profile curvature	0.658	1.519	Lithology	0.907	1.103	Distance to stream	0.393	2.543
Annual mean rainfall	0.547	1.828	LS factor	0.444	2.250	Land use	0.803	1.245
Aspect	0.917	1.091	Topographic wetness index	0.494	2.022	Lithology	0.818	1.222
			Profile curvature	0.604	1.657	Profile curvature	0.582	1.719
			Aspect	0.985	1.016			

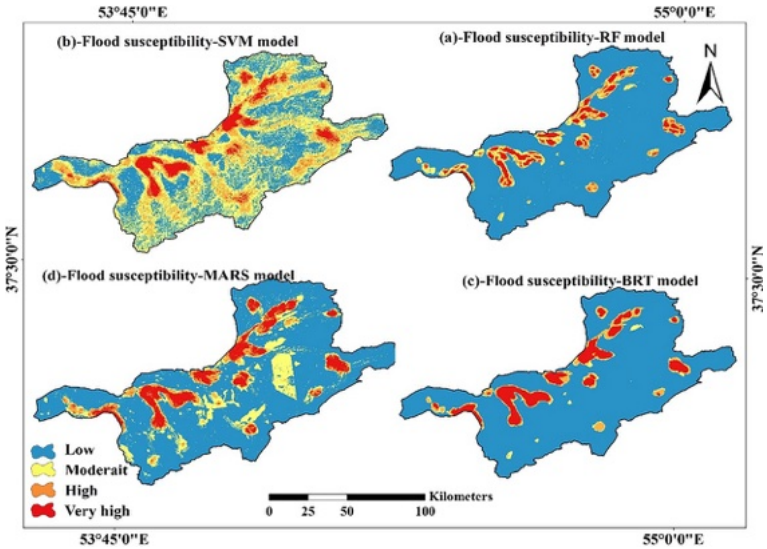

Fig. 4 Flood susceptibility maps produced using: **a** RF model; **b** SVM model; **c** BRT model; **d** MARS model

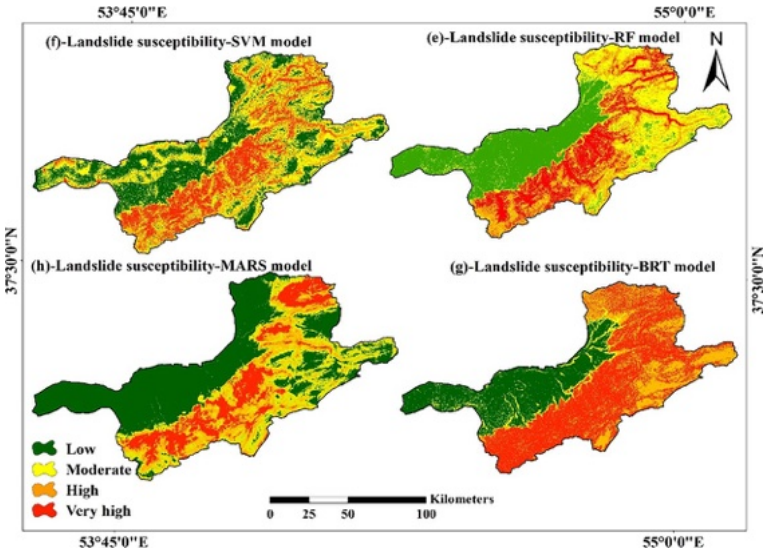

Fig. 5 Landslide susceptibility maps produced using: **a** RF model; **b** SVM model; **c** BRT model; **d** MARS model

of its upper and lower limits. As a pessimistic criterion in the validation process, Kappa coefficient values showed good performance for flood and trench erosion risk and moderate performance for landslide.

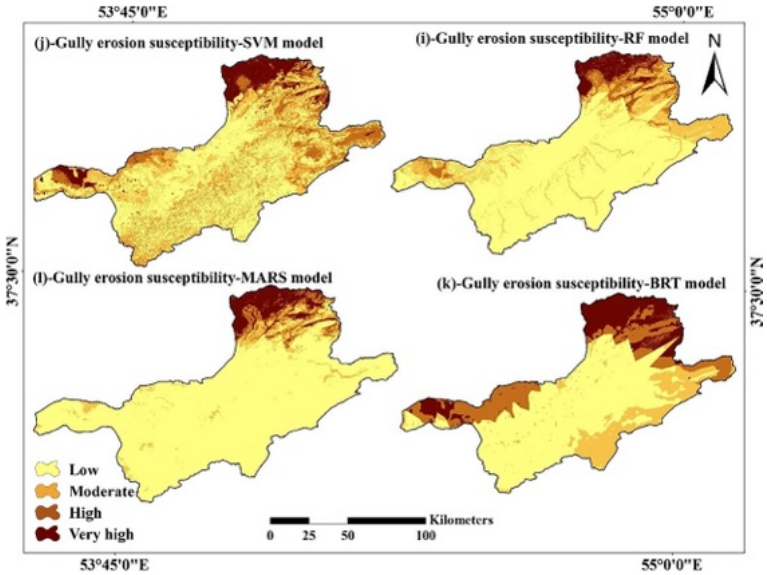

Fig. 6 Gully erosion susceptibility maps produced using: **a** RF model; **b** SVM model; **c** BRT model; **d** MARS model

4 Discussion

The most important causes of multiple hazards in the Gorganrood watershed are the mountainous nature of the region, the presence of landslide-prone lithology units, seasonal and circadian temperature differences, heavy rains, and human interference in the natural environment. The selection of the study area for this research, focused on susceptibility mapping of gully erosion, landslide, and flood hazards, was based on several key considerations. These include the historical occurrence of these hazards, the availability of relevant data, and the potential impact of the study on enhancing hazard mitigation strategies in the region. Gully erosion, a significant hazard in the study area, is influenced by various factors. These include soil texture, land cover changes, rainfall patterns, and topographic characteristics. The interaction of these factors plays a crucial role in the initiation and propagation of gullies, impacting the overall vulnerability of the landscape. Building upon the discussion of gully erosion factors, it is important to consider how these factors interplay with those influencing landslide hazards. The transition from gully erosion to landslide involves a shift in focus towards slope stability, geological conditions, land use practices, and precipitation as key drivers of landslide susceptibility in the study area. Landslide occurrence is governed by a complex interplay of factors, including slope, soil texture, land use, and lithology. By examining these factors in relation to the study area, a more comprehensive understanding of landslide hazard dynamics can be achieved, contributing to improved susceptibility mapping efforts. The discussion on landslide hazards naturally leads to an exploration of flood hazards, as landslides can significantly impact hydrological processes and increase flood risk. Factors such as channel morphology, land use changes, extreme precipitation events, and infrastructure development all contribute to the vulnerability of the study area to flooding, highlighting the interconnected nature of these hazards. In conclusion,

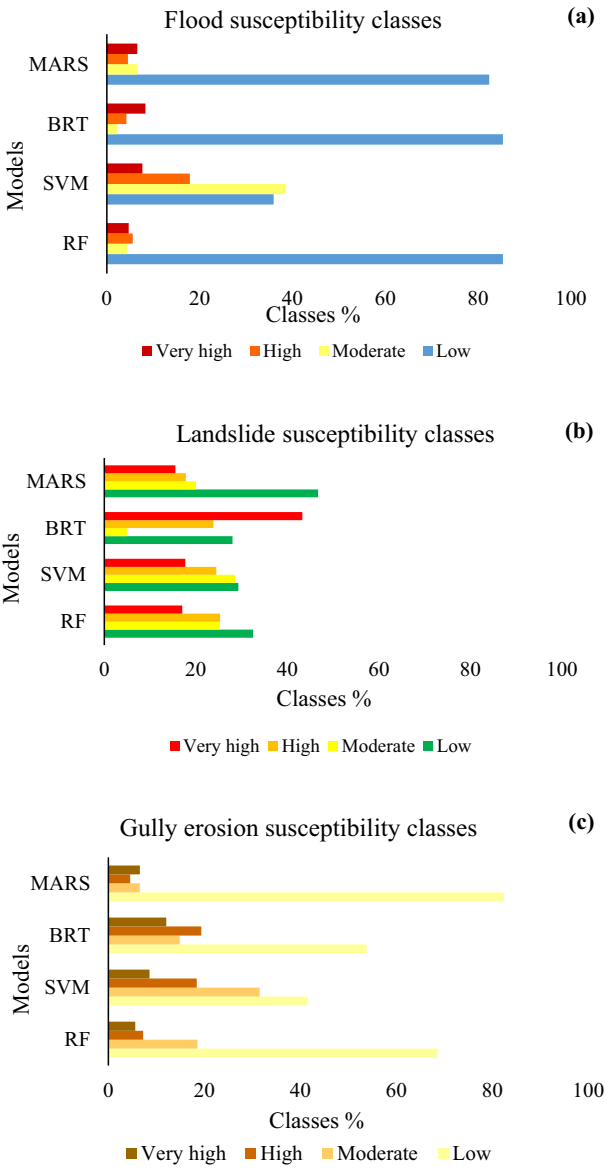

Fig. 7 Three hazards susceptibility distribution areas of the RF, SVM, BRT and MARS models: Floods (**a**); Landslide (**b**) and Gully erosion (**c**)

the integration of factors affecting gully erosion, landslides, and flood hazards is essential for developing comprehensive vulnerability maps and enhancing risk assessment strategies. By establishing clear transitions and organizing ideas cohesively, this study aims to provide a structured framework for understanding and addressing multiple hazards in the study area.

Based on the results obtained from Table 1, in relation to environmental factors, the highest percentage and amount of FR for FLGe hazards in Gorganrood watershed occurred in the following categories. The sections prone to gully erosion have sensitive lithology

Table 2 Statistical characteristics of the probability values obtained from RF, SVM, BRT and MARS models

Hazards	Models	Probabilistic prediction values	
		Mean	SD
Flood	RF	0.155	0.222
	SVM	0.236	0.248
	BRT	0.269	0.164
	MARS	0.139	0.259
Landslide	RF	0.313	0.229
	SVM	0.321	0.327
	BRT	0.438	0.115
	MARS	0.276	0.286
Gully erosion	RF	0.137	0.207
	SVM	0.174	0.269
	BRT	0.339	0.157
	MARS	0.109	0.245

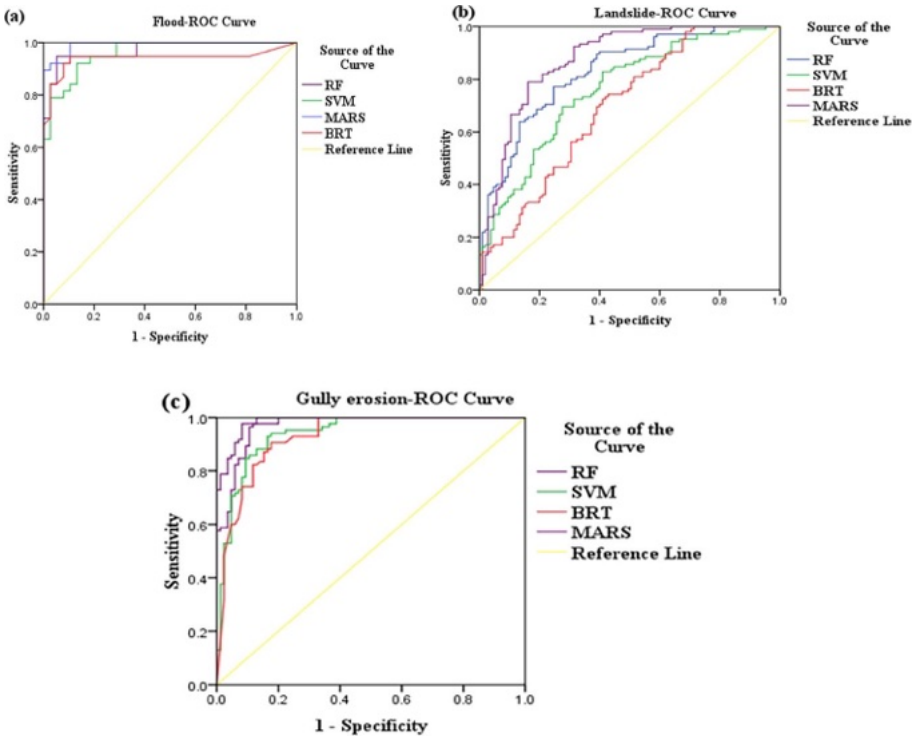

Fig. 8 ROC curves for three hazards (**a**) floods (**b**), landslide, and gullies (**c**)

(Quaternary sediments), soil texture, silty clay loam texture, and agricultural and rangeland use, and the annual rainfall was 384–549 mm. In addition, lowlands and south and southeast directions were observed at heights less than 500 m with a slope 26% >, SLC

Table 3 AUC values of validation data set

Three hazards	Models	Area	Standard error	Asymptotic significant	Asymptotic 95% confidence interval	
					Lower bound	Upper bound
Flood	RF	0.972	0.016	0.000	0.940	1.004
	SVM	0.961	0.018	0.000	0.924	0.997
	BRT	0.940	0.007	0.000	0.978	1.004
	MARS	0.991	0.000	0.000	0.874	1.006
Landslide	RF	0.829	0.028	0.000	0.774	0.833
	SVM	0.760	0.033	0.000	0.696	0.824
	BRT	0.695	0.036	0.000	0.624	0.765
	MARS	0.874	0.025	0.000	0.826	0.922
Gully erosion	RF	0.969	0.011	0.000	0.947	0.991
	SVM	0.939	0.018	0.000	0.904	0.974
	BRT	0.926	0.020	0.000	0.886	0.965
	MARS	0.985	0.06	0.000	0.973	0.998

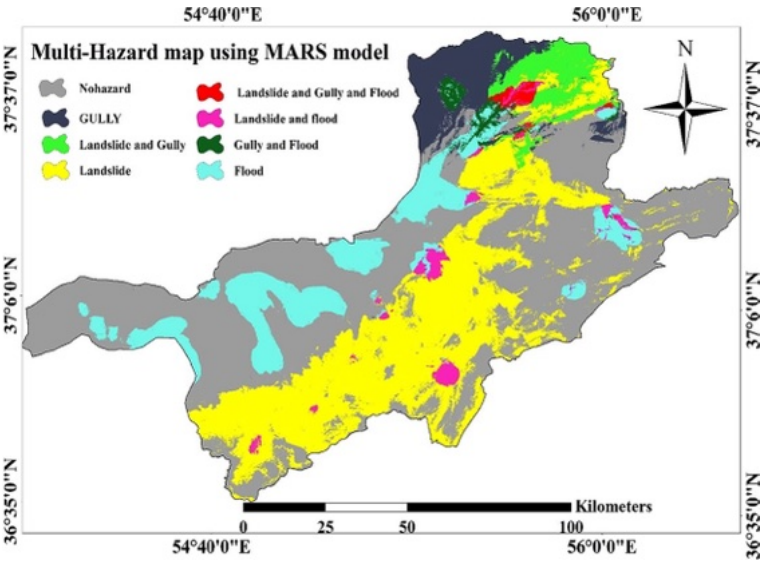

Fig. 9 Multi-hazard map produced by MARS model synthesizing the three hazard maps

0.01 >, TSC 0.01 <, drainage density 0–0.067 km/km^2, RSP 0–0.164, TWI 5.12–7.33, SPI 0–1343.97.

Landslide prone areas at an altitude of 807–1418 m with slopes above 45%, less than 4000 m from the fault, less than 900 m from the road, 1774 m distance from stream network, Qft group lithology, Delichai Formation (Murmg), soil texture Silty clay loam and silty loam, SPI 0–1343.97, TWI 1.20–5.12, RSP 0–0.164, drainage density 0.067–0.6,

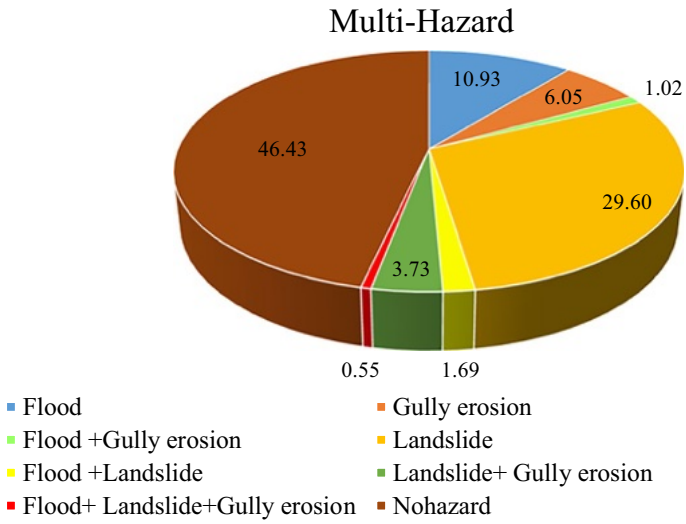

Fig. 10 Pie diagram of percentage of the study area predicted by MARS model to have combinations of FLGe

Table 4 Evaluating prediction performance of MARS model as the superior model

	Hazards		
	Flood	Landslide	Gully erosion
Sensitivity (%)	95.50	89/09	83.37
Specificity (%)	89.00	55.27	69.02
Efficiency (%)	46.5	46.2	43.2
Positive predictive value (NPP) (%)	89.16	66.58	72.91
Negative predictive value (NPV) (%)	90.36	83.52	80.58
Kappa coefficient	0.79	0.44	0.52

annual rainfall 608.21–810.28, SLC < 0.01, TSC < 0.01, forest land use and west slope direction were among the areas prone to landslide.

In areas with a height of – 95 to 296 and slope of less than 10%, agricultural land use, distance from stream network less than 3725 m, SLC − 0.01 to 0.01, TSC more than 0.01, annual rainfall 549.76–609.21, drainage density value 0.268–0.557 km/km^2, relative slope position 0–0.164, TWI 5.33–7.32, SPI 0–1343/97, silt loam soil texture and lithology of Qsw group, due to the concentration of surface and subsurface flows in the region towards stream and rivers, floods are most likely to occur. Drainage density factors (49.4%), digital elevation model (30.5%), and rainfall (41.7%) were identified as the most important environmental factors affecting the occurrence of FLGe in the study area. In addition, the variables of distance from stream network and lithology for flood risk, lithology and distance from fault for landslide risk, and digital elevation and land use model were important for trench erosion risk analysis. 77.52% of flooding occurs in areas with a drainage density between 0.557 and 0.268 km/km^2. Slope maps for SLCs and TSCs have been prepared

from digital elevation model maps; therefore, they are very important in modeling and determining areas prone to natural hazards. In Gorganrood watershed, 49.19% of landslide in areas with a height of 807–1418 m, which have slopes of 26.07–45.29%, have been landslide prone areas. Although surface landslide occur on steep slopes, the frequency of their occurrence is mostly lower on slopes greater than 45° (Dai et al. 2001; Sidel and Ochiai 2006). Areas with a height of less than 200 m and a slope of more than 26% are more prone to this type of erosion, and approximately 90% of gullies are located in this area, which can be attributed to the presence of vegetation (Daba et al. 2003). According to Chen and Yu (2011), the areas in the lower reaches have a larger upstream participation area and surface currents, which are more conducive to flooding, gully erosion, or landslide. Jokar Sarhangi and Khalkhali (2019), analysis of the role of altitude and slope factors in landscaping confirm this result.

Low slope areas are more susceptible to gullies and flooding. These results suggest a close relationship between the occurrence of gullies and floods on low slopes due to the infiltration of surface currents and the formation of tunnel or piping erosion. Kakembo et al. (2009) examined the influence of topographic thresholds (slope, curvature, and topographic position) on the occurrence of gullies. The occurrence of gullies is very complex due to several environmental factors (topography, geology, soil, etc.) that need to be controlled. As the slope of the ground increases, the thickness of loose material and alluvial deposits decreases and the likelihood of gully erosion decreases (Vanwalleghem et al. 2005; Zhang et al. 2023a, b).

Rainfall is considered to be one of the stimulus factors for erosion. During the process of water infiltration into the soil, the suction of the material is gradually reduced, and hence, the shear strength of the material is reduced, leading to soil erosion (Hong et al. 2016; Zhang et al. 2023a, b). The highest frequency ratio of gully erosion is 348–500 mm per year. Distance from stream network is one of the most important environmental variables that affect the magnitude and speed of floods (Band et al. 2020). The stability of a domain is controlled by saturating the material on the domain (Yalcin et al. 2011). Floods are most likely to occur close to the river in the study area. This may be due to the concentration of surface and subsurface flows towards streams and rivers in the region. Lithology plays a very important role in determining sensitivity, and different lithological units show significant differences in slope instability. Analysis of lithological classes in the study area shows that the Qsw and Qft groups with alluvial terrace formations have the highest susceptibility to floods and moat erosion, respectively (Avni. 2005).

Changes in land-use conditions lead to natural imbalances and instability (Sidel and Ochiai 2006; Prokopová et al. 2019). On the basis of land use results, one of the most important factors affecting gully erosion has been identified, which agrees with Samani et al. (2016) study. In addition, watersheds, whose predominant use is agricultural lands with gullies, have produced more sediments and floods than forest areas, even with landslide (Lesschen et al. 2007; Haregeweyn et al. 2017). According to the variables importance analysis, drainage density (89.4%), digital elevation model (30.5%), and rainfall (41.7%) were consistently highly ranked variables for flood, landslide, and gully erosion, respectively. These findings are consistent with Nohegar and Heydarzadeh (2011), Servati et al. (2014), Bui et al. (2016a), Khosravi et al. (2016), Lee et al. (2007), and Azareh et al. (2019) studies. The results showed that the model predictions based on all these flood risk criteria were better than those based on the landslide and gully erosion criteria. Variables that affect the occurrence of natural hazards in one region may be different from other regions due to different topological, climatic, hydrological, geomorphological, soil and human factors (Barman et al. 2024). Landslides have occurred around rivers in some areas,

and distance from the stream network is a major cause (Demir et al. 2015). Landslide caused by human factors around the roads were the main cause of distance from the road (Zhang et al. 2024), and based on the research results, it is not possible to suggest a method for all the regions (Chen et al. 2017; Pourghasemi and Rahmati. 2018).

5 Conclusion

In this study, RF, SVM, BRT, and MARS models were used to identify areas prone to FLGe in the Gorganrood watershed, record the locations of 283 gully erosion points, 351 landslide points, and 127 flood points in the region, and obtain forecast maps of areas susceptible to FLGe. The utilization of RF, SVM, BRT, and MARS models in susceptibility mapping for gully erosion, landslide, and floods within the Gorganrood watershed has yielded crucial insights into the spatial distribution of these hazards. The identification of high-risk areas, particularly in sloping and high regions for landslide and the alluvial and flat central parts for floods, underscores the importance of targeted risk mitigation strategies. The findings highlight the complex interplay of topographical, hydrological, and land use factors in shaping the vulnerability landscape of the watershed.

According to the model maps, sloping and high areas have high and low occurrence potentials for landslide and gully erosion, respectively, and alluvial and flat central parts adjacent to surface currents have a moderate to high flood risk. The SVM, BRT, and MARS models had the highest landslide risk in the very high class in the random RF model. Each model showcased unique strengths and limitations in capturing the nuances of hazard occurrence, emphasizing the need for a multi-model approach to enhance the accuracy and reliability of risk mapping efforts. Understanding the specific capabilities and constraints of each model can inform decision-makers on selecting the most appropriate tool for their risk assessment needs. The results show that approximately 50% of the Gorganrood watershed is at risk and that some of these areas fall within a multi-risk category and are therefore susceptible to more than one risk. This map makes it possible to identify multiple risk areas.

Based on the study's findings, key recommendations can be formulated to guide decision-makers, policymakers, and researchers in enhancing risk mitigation and management strategies. These recommendations may encompass improved land use planning practices, early warning systems implementation, and targeted infrastructure development to minimize the impact of hazards on vulnerable communities. Additionally, fostering interdisciplinary collaborations and investing in continuous monitoring and data collection efforts can bolster preparedness and response mechanisms in the face of evolving hazard dynamics. he identification of areas susceptible to multiple hazards underscores the complexity and interconnected nature of hazard occurrences within the watershed. Managing such multi-risk scenarios necessitates a holistic and adaptive approach that integrates cross-sectoral expertise, community engagement, and innovative risk communication strategies. Addressing the challenges associated with overlapping hazards requires tailored interventions that prioritize resilience-building measures, sustainable land use practices, and ecosystem-based solutions to mitigate the cascading effects of disasters. In conclusion, the study's comprehensive analysis of hazard vulnerabilities in the Gorganrood watershed offers valuable insights into the spatial dynamics of gully erosion, landslide, and flood. By providing actionable recommendations and highlighting the significance of multi-risk areas, this research contributes to the ongoing dialogue on effective risk management

strategies and underscores the importance of proactive measures in enhancing community resilience to natural hazards.

Acknowledgements We would like to express our gratitude to all individuals and organizations who provided valuable assistance and support during the fieldwork and research activities conducted for this study. Their contributions were instrumental in the successful completion of this project. We acknowledge their dedication and collaborative efforts in enhancing the quality and reliability of our findings.

Authors' contributions The authors of this paper have made significant and collective contributions to the conceptualization, methodology development, data analysis, and interpretation of results. Each author played a crucial role in different stages of the research process, contributing their expertise and insights to ensure the rigor and validity of the study outcomes. Their collaborative efforts have been essential in advancing our understanding of vulnerability mapping for gully erosion, landslide, and flood hazards.

Funding Funding is provided by Sari Agricultural Sciences and Natural Resources University.

Declarations

Conflict of interest The authors declare to not have any potential conflicts of interest. In this research, human participants and/or animals were not included.

References

Aksha SK, Resler LM, Juran L, Carstensen LW (2020) A geospatial analysis of multi-hazard risk in Dharan, Nepal. Geomat Nat Hazards Risk 11(1):88–111. https://doi.org/10.1080/19475705.2019.1710580

Al Mamun A, Islam ARMT, Alam GM, Sarker MNI, Erdiaw-Kwasie MO, Bhandari H, Mallick J (2023) Livelihood vulnerability of char land communities to climate change and natural hazards in Bangladesh: an application of livelihood vulnerability index. Nat Hazards 115(2):1411–1437

Alqadhi S, Mallick J, Talukdar S, Bindajam AA, Van Hong N, Saha TK (2022) Selecting optimal conditioning parameters for landslide susceptibility: an experimental research on Aqabat Al-Sulbat, Saudi Arabia. Environ Sci Oollut R 29(3):3743–3762

Arabameri A, Rezaei K, Cerdà A, Conoscenti C, Kalantari Z (2019) A comparison of statistical methods and multi-criteria decision making to map flood hazard susceptibility in Northern Iran. Sci Total Environ 660:443–458. https://doi.org/10.1016/j.scitotenv.2019.01.021

Avand M, Janizadeh S, Naghibi SA, Pourghasemi HR, Khosrobeigi Bozchaloei S, Blaschke T (2019) A comparative assessment of random forest and k-nearest neighbor classifiers for gully erosion susceptibility mapping. Water 11(10):2076. https://doi.org/10.3390/w11102076

Avni Y (2005) Gully incision as a key factor in desertification in an arid environment, the Negev highlands, Israel. CATENA 63(2–3):185–220. https://doi.org/10.1016/j.catena.2005.06.004

Azareh A, Rahmati O, Rafiei-Sardooi E, Sankey JB, Lee S, Shahabi H, Ahmad BB (2019) Modelling gully-erosion susceptibility in a semi-arid region, Iran: investigation of applicability of certainty factor and maximum entropy models. Sci Total Environ 655:684–696. https://doi.org/10.1016/j.scitotenv.2018.11.235

Band SS, Janizadeh S, Chandra Pal S, Saha A, Chakrabortty R, Melesse AM, Mosavi A (2020) Flash flood susceptibility modeling using new approaches of hybrid and ensemble tree-based machine learning algorithms. Remote Sens 12(21):3568. https://doi.org/10.3390/rs12213568

Barman J, Biswas B, Rao KS (2024) A hybrid integration of analytical hierarchy process (AHP) and the multiobjective optimization on the basis of ratio analysis (MOORA) for landslide susceptibility zonation of Aizawl, India. Nat Hazards 8:1–26

Bathrellos GD, Skilodimou HD, Chousianitis K, Youssef AM, Pradhan B (2017) Suitability estimation for urban development using multi-hazard assessment map. Sci Total Environ 575:119–134. https://doi.org/10.1016/j.scitotenv.2016.10.025

Brito MMD, Evers M, Almoradie ADS (2018) Participatory flood vulnerability assessment: a multi-criteria approach. Hydrol Earth Syst Sci 22(1):373–390. https://doi.org/10.5194/hess-22-373-2018,2018

Bui DT, Pradhan B, Nampak H, Bui QT, Tran QA, Nguyen QP (2016a) Hybrid artificial intelligence approach based on neural fuzzy inference model and metaheuristic optimization for flood

susceptibilitgy modeling in a high-frequency tropical cyclone area using GIS. J Hydrol 540:317–330. https://doi.org/10.1016/j.jhydrol.2016.06.027
Bui DT, Tuan TA, Klempe H, Pradhan B, Revhaug I (2016b) Spatial prediction models for shallow landslide hazards: a comparative assessment of the efficacy of support vector machines, artificial neural networks, kernel logistic regression, and logistic model tree. Landslides 13(2):361–378
[CONRWMGP] Central Office of Natural Resources and Watershed Management in Golestan Province (2009) Detailed action plan, Iran, p 230
Chen CY, Yu FC (2011) Morphometric analysis of debris flows and their source areas using GIS. Geomorphology 129(3–4):387–397. https://doi.org/10.1016/j.geomorph.2011.03.002
Chen W, Xie X, Wang J, Pradhan B, Hong H, Bui DT, Duan Z, Ma J (2017) A comparative study of logistic model tree, random forest, and classification and regression tree models for spatial prediction of landslide susceptibility. CATENA 151:147–160. https://doi.org/10.1016/j.catena.2016.11.032
Conforti M, Aucelli PP, Robustelli G, Scarciglia F (2011) Geomorphology and GIS analysis for mapping gully erosion susceptibility in the Turbolo stream catchment (Northern Calabria, Italy). Nat Hazards 56(3):881–898
Conoscenti C, Agnesi V, Angileri S, Cappadonia C, Rotigliano E, Marker M (2013) A GIS-based approach for gully erosion susceptibility modeling: a test in Sicily. Italy Environ Earth Sci 70(3):1179–1195
Conoscenti C, Angileri S, Cappadonia C, Rotigliano E, Agnesi V, Märker M (2014) Gully erosion susceptibility assessment by means of GIS-based logistic regression: a case of Sicily (Italy). Geomorphology 204:399–411. https://doi.org/10.1016/j.geomorph.2013.08.021
Costache R, Hong H, Pham QB (2020) Comparative assessment of the flash-flood potential within small mountain catchments using bivariate statistics and their novel hybrid integration with machine learning models. Sci Total Environ 711:134514. https://doi.org/10.1016/j.scitotenv.2019.134514
Costache R, Pal SC, Pande CB, Islam ARMT, Alshehri F, Abdo HG (2024) Flood mapping based on novel ensemble modeling involving the deep learning, Harris Hawk optimization algorithm and stacking based machine learning. Appl Water Sci 14(4):78
Daba S, Rieger W, Strauss P (2003) Assessment of gully erosion in eastern Ethiopia using photogrammetric techniques. CATENA 50(2–4):273–291. https://doi.org/10.1016/S0341-8162(02)00135-2
Dai FC, Lee CF, Li JXZW, Xu ZW (2001) Assessment of landslide susceptibility on the natural terrain of Lantau Island, Hong Kong. Environ Geol 40(3):381–391
Daoud JI (2017) Multicollinearity and regression analysis. J Phys Conf Ser 949(1):012009
Demir G, Aytekin M, Akgun A (2015) Landslide susceptibility mapping by frequency ratio and logistic regression methods: an example from Niksar-Resadiye (Tokat, Turkey). Arab J Geosci 8(3):1801–1812. https://doi.org/10.1007/s12517-014-1332-z
Devkota KC, Regmi AD, Pourghasemi HR, Yoshida K, Pradhan B, Ryu IC, Raj Dhital M, Althuwaynee OF (2013) Landslide susceptibility mapping using certainty factor, index of entropy and logistic regression models in GIS and their comparison at Mugling-Narayanghat road section in Nepal Himalaya. Nat Hazards 65(1):135–165
El Morjani ZEA, Ebener S, Boos J, Ghaffar EA, Musani A (2007) Modelling the spatial distribution of five natural hazards in the context of the WHO/EMRO Atlas of Disaster Risk as a step towards the reduction of the health impact related to disasters. Int J Health Geogr 6(1):8
El-Magd A, Ahmed S (2022) Random forest and naïve Bayes approaches as tools for flash flood hazard susceptibility prediction, South Ras El-Zait, Gulf of Suez Coast, Egypt. Arab J Geosci 15(3):1–12
FelicÍsimo Á, Cuartero A, Remondo J, Quirós E (2013) Mapping landslide susceptibility with logistiv regression, multiple adaptive regression splines, classification and regression tress, amd maximum entropy methods: a comparative study. Landslides 10:175–189
Ganesh B, Vincent S, Pathan S, Benitez SRG (2023) Integration of GIS and machine learning techniques for mapping the landslide-prone areas in the state of Goa, India. J Indian Soc Remote Sens 51:1–13
Gayen A, Haque SM, Saha S (2020) Modeling of gully erosion based on random forest using GIS and R. Gully erosion studies from India and surrounding regions. Springer, Cham, pp 35–44
Ge W, Deng L, Wang F, Han J (2021) Quantifying the contributions of human activities and climate change to vegetation net primary productivity dynamics in China from 2001 to 2016. Sci Total Environ 773:145648. https://doi.org/10.1016/j.scitotenv.2021.145648
Gill JC, Malamud BD (2014) Reviewing and visualizing the interactions of natural hazards. Rev Geophys 52:680–722
Gnyawali K, Dahal K, Talchabhadel R, Nirandjan S (2023) Framework for rainfall-triggered landslide-prone critical infrastructure zonation. Sci Total Environ 872:162242. https://doi.org/10.1016/j.scitotenv.2023.162242
Greene WH (2000) Econometric analysis, 4th edn. Prentice Hall, Upper Saddle River

Guzzetti F, Cardinali M, Reichenbach P, Carrara A (2000) Comparing landslide maps: a case study in the Upper Tiber River Basin, Central Italy. Environ Manag 25:3. https://doi.org/10.1007/s002679910020
Hai T, Theruvil Sayed B, Majdi A, Zhou J, Sagban R, Band SS, Mosavi A (2023) An integrated GIS-based multivariate adaptive regression splines-cat swarm optimization for improving the accuracy of wildfire susceptibility mapping. Geocarto Int. https://doi.org/10.1080/10106049.2023.2167005
Haregeweyn N, Tsunekawa A, Poesen J, Tsubo M, Meshesha DT, Fenta AA, Nyssen J, Adgo E (2017) Comprehensive assessment of soil erosion risk for better land use planning in river basins: case study of the Upper Blue Nile River. Sci Total Environ 574:95–108. https://doi.org/10.1016/j.scitotenv.2016.09.019
Hong H, Pradhan B, Xu C, Bui DT (2015) Spatial prediction of landslide hazard at the Yihuang area (China) using two-class kernel logistic regression, alternating decision tree and support vector machines. CATENA 133:266–281. https://doi.org/10.1016/j.catena.2015.05.019
Hong H, Pradhan B, Jebur MN, Bui DT, Xu C, Akgun A (2016) Spatial prediction of landslide hazard at the Luxi area (China) using support vector machines. Environ Earth Sci 75(1):1–14
Islam ARMT, Talukdar S, Mahato S, Kundu S, Eibek KU, Pham QB, Kuriqi A, Linh NTT (2021) Flood susceptibility modelling using advanced ensemble machine learning models. Geosci Front 12(3):101075. https://doi.org/10.1016/j.gsf.2020.09.006
Javidan N, Kavian A, Pourghasemi HR, Conoscenti C, Jafarian Z (2020) Gully erosion susceptibility mapping using multivariate adaptive regression splines—replications and sample size scenarios. Water 11(11):2319. https://doi.org/10.3390/w11112319
Jokar Sarhangi E, Khalkhali N (2019) Evaluation and zonation the gully erosion hazard using bivariate statistical methods (case study: Nemarestagh Watershed). Environ Hazards 8(19):195–208
Kakembo V, Xanga WW, Rowntree K (2009) Topographic thresholds in gully development on the hillslopes of communal areas in Ngqushwa Local Municipality, Eastern Cape, South Africa. Geomorphology 110(3–4):188–194. https://doi.org/10.1016/j.geomorph.2009.04.006
Kalantar B, Pradhan B, Naghibi SA, Motevalli A, Mansor S (2018) Assessment of the effects of training data selection on the landslide susceptibility mapping: a comparison between support vector machine (SVM), logistic regression (LR) and artificial neural networks (ANN). Geomat Nat Hazards Risk 9(1):49–69. https://doi.org/10.1080/19475705.2017.1407368
Karaman H (2015) Integrated multi-hazard map creation by using AHP and GIS. Geomatics Engineering Department, Istanbul Technical University, Recent Advances on Environmental and Life Science
Kavian A, Hoseinpoor Sabet S, Solaimani K, Jafari B (2017) Simulating the effects of land use changes on soil erosion using RUSLE model. Geocarto Int 32(1):97–111. https://doi.org/10.1080/10106049.2015.1130083
Kavian A, Mirzaei SN, Choubin B, Kalehhouei M, Rodrigo-Comino J (2023) Mapping sediment mobilization risks: prioritizing results obtained at watershed and sub-watershed scales. Int Soil Water Conserv Res. https://doi.org/10.1016/j.iswcr.2023.09.003
Khosravi K, Nohani E, Maroufinia E, Pourghasemi HR (2016) A GIS-based flood susceptibility assessment and its mapping in Iran: a comparison between frequency ratio and weights-of-evidence bivariate statistical models with multi-criteria decision-making technique. Nat Hazards 83(2):947–987
Komac M (2006) A landslide susceptibility model using the analytical hierarchy process method and multivariate statistics in perialpine Slovenia. Geomorphology 74:17–28. https://doi.org/10.1016/j.geomorph.2005.07.005
Kornejady A, Ownegh M, Bahremand A (2017) Landslide susceptibility assessment using maximum entropy model with two different data sampling methods. CATENA 152:144–162. https://doi.org/10.1016/j.catena.2017.01.010
Kourtit K, Nijkamp P, Banica A (2023) An analysis of natural disasters' effects—a global comparative study of 'blessing in disguise.' Socioecon Plann Sci. https://doi.org/10.1016/j.seps.2023.101599
Lee S, Ryu JH, Kim IS (2007) Landslide susceptibility analysis and its verification using likelihood ratio, logistic regression, and artificial neural network models: case study of Youngin, Korea. Landslides 4(4):327–338
Lesschen JP, Kok K, Verburg PH, Cammeraat LH (2007) Identification of vulnerable areas for gully erosion under different scenarios of land abandonment in Southeast Spain. CATENA 71(1):110–121. https://doi.org/10.1016/j.catena.2006.05.014
Li Z, Yin C, Tan Z, Liu X, Li S, Ma X, Zhang X (2024) Landslide susceptibility assessment considering time-varying of dynamic factors. Nat Hazards Rev 25(3):05024004
Marjanović M, Kovačević M, Bajat B, Voženílek V (2011) Landslide susceptibility assessment using SVM machine learning algorithm. Eng Geol 123(3):225–234. https://doi.org/10.1016/j.enggeo.2011.09.006
Micheletti N, Foresti L, Robert S, Leuenberger M, Pedrazzini A, Jaboyedoff M, Kanevski M (2014) Machine learning feature selection methods for landslide susceptibility mapping. Math Geosci 46(1):33–57. https://doi.org/10.1007/s11004-013-9511-0

Moghaddam DD, Pourghasemi HR, Rahmati O (2019) Assessment of the contribution of geo-environmental factors to flood inundation in a semi-arid region of SW Iran: comparison of different advanced modeling approaches. Natural hazards GIS-based spatial modeling using data mining techniques. Springer, Cham, pp 59–78

Nanda AM, Lone FA, Ahmed P (2024) Prediction of rainfall-induced landslide using machine learning models along highway Bandipora to Gurez road, India. Nat Hazards 6:1–29

Nohegar A, Heydarzadeh M (2011) The study of physical-chemical characteristics and morphometery of gullying area (case study: Gezir, Hormozgan province)

Norouzi G, Taslimi M (2012) The impact of flood damages on production of Iran's Agricultural Sector. Middle East J Sci Res 12:921–926. https://doi.org/10.5829/idosi.mejsr.2012.12.7.1783

Nyantakyi-Frimpong H, Dinko DH, Kerr RB (2023) Floodplain farming and maladaptation to extreme rainfall events in northern Ghana. Clim Dev 15(3):201–214. https://doi.org/10.1080/17565529.2022.2074953

Pourghasemi HR, Rahmati O (2018) Prediction of the landslide susceptibility: which algorithm, which precision? CATENA 162:177–192. https://doi.org/10.1016/j.catena.2017.11.022

Pourghasemi HR, Gayen A, Park S, Lee CW, Lee S (2018) Assessment of landslide prone areas and its zonation using logistic regression, Logit Boost, and NaïveBayes machine learning algorithms. Sustainability 10(10):3697. https://doi.org/10.3390/su10103697

Pourghasemi HR, Gayen A, Panahi M, Rezaie F, Blaschke T (2019) Multi-hazard probability assessment and mapping in Iran. Sci Total Environ 692:556–571. https://doi.org/10.1016/j.scitotenv.2019.07.203

Prokopová M, Salvati L, Egidi G, Cudlín O, Včeláková R, Plch R, Cudlín P (2019) Envisioning present and future land-use change under varying ecological regimes and their influence on landscape stability. Sustainability 11(17):4654. https://doi.org/10.3390/su11174654

Rahmati O, Haghizadeh A, Pourghasemi HR, Noormohamadi F (2016) Gully erosion susceptibility mapping: the role of GIS-based bivariate statistical models and their comparison. Nat Hazards 82(2):1231–1258

Raji SA, Akintuyi AO, Wunude EO, Fashoto B (2023) A machine learning-based spatial statistical method for modelling different phases of gully development in South-Eastern Nigeria. Ecol Inform 75:102101. https://doi.org/10.1016/j.ecoinf.2023.102101

Samani AN, Chen Q, Khalighi S, Wasson RJ, Rahdari MR (2016) Assessment of land use impact on hydraulic threshold conditions for gully head cut initiation. Hydrol Earth Syst Sci 20(7):3005–3012

Sameen MI, Pradhan B, Bui DT, Alamri AM (2020) Systematic sample subdividing strategy for training landslide susceptibility models. CATENA 187:104358

Sari AR (2023) The impact of good governance on the quality of public management decision making. Contemp Manag Res (ADMAN) 1(2):39–46. https://doi.org/10.61100/adman.v1i2.21

Servati MR, Ghahrodi Tali M, Golkarami A, Njafi E (2014) Geomorphological thresholds for gully erosion in Kchick watershed, NE Golestan Province. J Geogr Sci 32:231–249

Sheikh V, Kornejady A, Ownegh M (2019) Application of the coupled TOPSIS-Mahalanobis distance for multi-hazard-based management of the target districts of the Golestan Province, Iran. Nat Hazards 96(3):1335–1365

Shi W, Chen G, Meng X, Bian S, Jin J, Wu J, Huang F, Chong Y (2023) Formation and hazard analysis of landslide damming based on multi-source remote sensing data. Remote Sens 15(19):4691

Sidel RC, Ochiai H (2006) Landslides: processes, prediction, and land use, water resource monograph, 18th edn. AGU Books

Soulard CE, Acevedo W, Stehman SV, Parker OP (2016) Mapping extent and change in surface mines within the United States for 2001 to 2006. Land Degrad Dev 27(2):248–257. https://doi.org/10.1002/ldr.2412

UNEP (1992) Agenda 21. Technical Report. United Nations Environment Programme. http://www.un.org/esa/dsd/agenda21/res_agenda21_07.shtml. Accessed 3 Sept 2009

United Nations Office for Disaster Risk Reduction (2005) National report of the Islamic Republic of Iran. World Conference on Disaster Reduction, Kobe, Hyogo, Japan

Vanwalleghem T, Poesen J, Nachtergaele J, Verstraeten G (2005) Characteristics, controlling factors and importance of deep gullies under cropland on loess-derived soils. Geomorphology 69(1–4):76–91. https://doi.org/10.1016/j.geomorph.2004.12.003

Wang X, Wen Z, Liu G, Tao H, Song K (2022) Remote estimates of total suspended matter in China's main estuaries using Landsat images and a weight random forest model. ISPRS J Photogramm Remote Sens 183:94–110. https://doi.org/10.1016/j.isprsjprs.2021.11.001

Water Resources Company of Golestan [WRCG] (2013) Precipitation and temperature reports; [cited 2013 August 11]. Available from: http://www.gsrw.ir/Default.aspx

Widantara KW, Mutaqin BW (2024) Multi-hazard assessment in the coastal tourism city of Denpasar, Bali, Indonesia. Nat Hazards 8:1–34

Yalcin A, Reis S, Aydinoglu AC, Yomralioglu T (2011) A GIS-based comparative study of frequency ratio, analytical hierarchy process, bivariate statistics and logistics regression methods for landslide susceptibility mapping in Trabzon, NE Turkey. CATENA 85(3):274–287. https://doi.org/10.1016/j.catena.2011.01.014

Yesilnacar E, Topal T (2005) Landslide susceptibility mapping: a comparison of logistic regression and neural networks methods in a medium scale study, Hendek region (Turkey). Eng Geol 79(3):251–266. https://doi.org/10.1016/j.enggeo.2005.02.002

Yesilnacar EK (2005) The application of computational intelligence to landslid susceptibility mapping in Turkey. Ph.D Thesis, Department of Geomatics the University of Melbourne, p 423

Youssef AM, Pourghasemi HR, Pourtaghi ZS, Al-Katheeri MM (2016) Landslide susceptibility mapping using random forest, boosted regression tree, classification and regression tree, and general linear models and comparison of their performance at Wadi Tayyah Basin, Asir Region, Saudi Arabia. Landslides 13:839–856

Zhang H, Liu G, Zhao C, Zhang L, Zhang Q, Fu H, Cao S (2023a) Loess erosion change modeling during heavy rainfall. Int J Sediment Res 38(1):24–32. https://doi.org/10.1016/j.ijsrc.2022.08.004

Zhang Z, Zeng R, Meng X, Zhao S, Wang S, Ma J, Wang H (2023b) Effects of changes in soil properties caused by progressive infiltration of rainwater on rainfall-induced landslides. CATENA 233:107475. https://doi.org/10.1016/j.catena.2023.107475

Zhang J, Cao Y, Fan W, Zheng W, Wang Z, He C, Teng H (2024) Spatial distribution characteristics and influence factor analysis of landslides—case study of the Hanwang area in Qinba Mountains. Earthq Res Adv. https://doi.org/10.1016/j.eqrea.2024.100275

Zhao G, Pang B, Xu Z, Yue J, Tu T (2018) Mapping flood susceptibility in mountainous areas on a national scale in China. Sci Total Environ 615:1133–1142. https://doi.org/10.1016/j.scitotenv.2017.10.037

Authors and Affiliations

Narges Javidan[1] · Ataollah Kavian[1] · Christian Conoscenti[2] · Zeinab Jafarian[3] · Mahin Kalehhouei[4] · Raana Javidan[5,6]

✉ Ataollah Kavian
a.kavian@sanru.ac.ir

[1] Department of Watershed Management, Faculty of Natural Resources, Sari Agricultural Sciences and Natural Resources University (SANRU), Sari 48441-74111, Iran

[2] Department of Earth and Marine Sciences (DISTEM), University of Palermo, 90123 Palermo, Italy

[3] Department of Range Management, Sari Agricultural Sciences and Natural Resources University (SANRU), Sari 48441-74111, Iran

[4] Department of Watershed Management Engineering, Faculty of Natural Resources, Tarbiat Modares University, Tehran, Iran

[5] Department of Environmental Engineering, Faculty of Natural Resources, University of Environment, Karaj, Iran

[6] Department of Environmental Engineering, Research Center of Environment and Sustainable Development, Karaj, Iran